Signal processing on spherical manifolds

Jason McEwen

http://www.jasonmcewen.org/

Department of Physics and Astronomy
University College London (UCL)

Probabilistic And Statistical techniques for Cosmological AnaLysis (PASCAL)
Rome :: June 2013

Observations on spherical manifolds
Cosmology

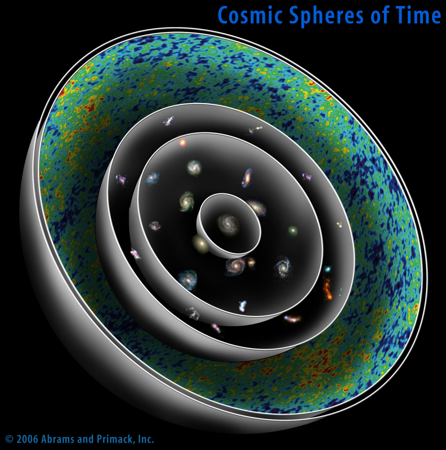

Cosmic microwave background (CMB)

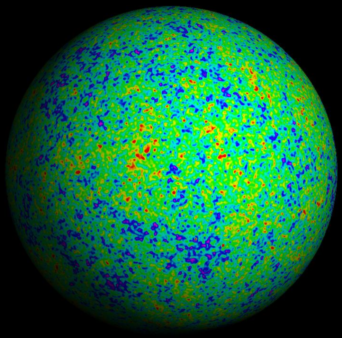

Credit: WMAP

Galaxy surveys

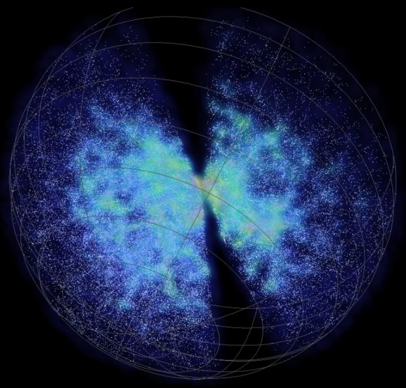

Credit: SDSS

Outline

Outline

Recall wavelet transform in Euclidean space

- Project signal onto wavelets

$$\mathcal{W}^f(a,b) = \langle f, \psi_{a,b} \rangle = |a|^{-1/2} \int_{-\infty}^{\infty} \mathrm{d}t \, f(t) \, \psi^*\left(\frac{t-b}{a}\right),$$

where

$$\psi_{a,b} = |a|^{-1/2} \psi\left(\frac{t-b}{a}\right).$$

- Synthesis signal from wavelet coefficients

$$f(t) = C_\psi^{-1} \int_{-\infty}^{\infty} \mathrm{d}b \int_0^{\infty} \frac{\mathrm{d}a}{a^2} \, \mathcal{W}^f(a,b) \psi_{a,b}(t).$$

- Admissibility condition to ensure perfect reconstruction

$$0 < C_\psi \equiv \int_{-\infty}^{\infty} \frac{\mathrm{d}k}{|k|} \, |\hat{\psi}(k)|^2 < \infty.$$

Recall wavelet transform in Euclidean space

- Project signal onto wavelets

$$\boxed{\mathcal{W}^f(a,b) = \langle f, \psi_{a,b} \rangle = |a|^{-1/2} \int_{-\infty}^{\infty} \mathrm{d}t \, f(t) \, \psi^* \left(\frac{t-b}{a} \right),}$$

where

$$\psi_{a,b} = |a|^{-1/2} \psi \left(\frac{t-b}{a} \right).$$

- Synthesis signal from wavelet coefficients

$$f(t) = C_\psi^{-1} \int_{-\infty}^{\infty} \mathrm{d}b \int_0^{\infty} \frac{\mathrm{d}a}{a^2} \, \mathcal{W}^f(a,b) \psi_{a,b}(t).$$

- Admissibility condition to ensure perfect reconstruction

$$0 < C_\psi \equiv \int_{-\infty}^{\infty} \frac{\mathrm{d}k}{|k|} \, |\hat{\psi}(k)|^2 < \infty.$$

Recall wavelet transform in Euclidean space

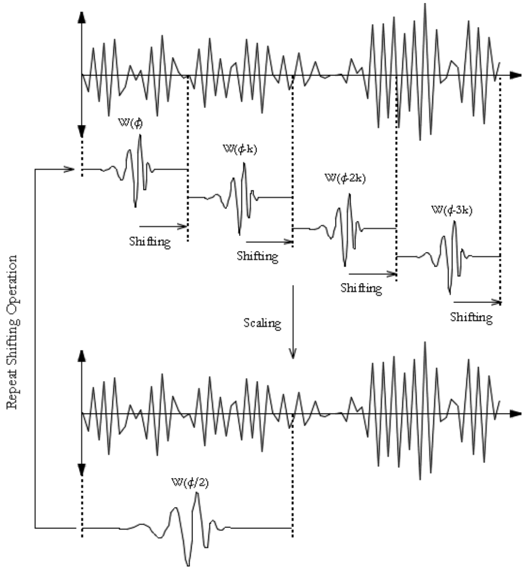

Figure: Wavelet scaling and shifting (Credit: `http://www.wavelet.org/tutorial/`)

Continuous wavelets on the sphere

- One of the first natural wavelet construction on the sphere was derived in the seminal work of Antoine and Vandergheynst (1998) (reintroduced by Wiaux 2005).
- Construct wavelet atoms from affine transformations (dilation, translation) on the sphere of a mother wavelet.
- The natural extension of translations to the sphere are rotations. Rotation of a function f on the sphere is defined by

$$[\mathcal{R}(\rho)f](\omega) = f(\rho^{-1} \cdot \omega), \quad \omega = (\theta, \varphi) \in \mathbb{S}^2, \quad \rho = (\alpha, \beta, \gamma) \in \mathrm{SO}(3) .$$

- How define dilation on the sphere?
- The spherical dilation operator is defined through the conjugation of the Euclidean dilation and stereographic projection Π:

$$\mathcal{D}(a) \equiv \Pi^{-1}\, d(a)\, \Pi .$$

Continuous wavelets on the sphere

- One of the first natural wavelet construction on the sphere was derived in the seminal work of Antoine and Vandergheynst (1998) (reintroduced by Wiaux 2005).
- Construct wavelet atoms from affine transformations (dilation, translation) on the sphere of a mother wavelet.
- The natural extension of translations to the sphere are rotations. Rotation of a function f on the sphere is defined by

$$[\mathcal{R}(\rho)f](\omega) = f(\rho^{-1} \cdot \omega), \quad \omega = (\theta, \varphi) \in \mathbb{S}^2, \quad \rho = (\alpha, \beta, \gamma) \in \mathrm{SO}(3) .$$

- How define dilation on the sphere?
- The spherical dilation operator is defined through the conjugation of the Euclidean dilation and stereographic projection Π:

$$\mathcal{D}(a) \equiv \Pi^{-1}\, d(a)\, \Pi .$$

Continuous wavelets on the sphere

- One of the first natural wavelet construction on the sphere was derived in the seminal work of Antoine and Vandergheynst (1998) (reintroduced by Wiaux 2005).
- Construct wavelet atoms from affine transformations (dilation, translation) on the sphere of a mother wavelet.
- The natural extension of translations to the sphere are rotations. Rotation of a function f on the sphere is defined by

$$[\mathcal{R}(\rho)f](\omega) = f(\rho^{-1} \cdot \omega), \quad \omega = (\theta, \varphi) \in \mathbb{S}^2, \quad \rho = (\alpha, \beta, \gamma) \in \mathrm{SO}(3) \ .$$

- How define dilation on the sphere?
- The spherical dilation operator is defined through the conjugation of the Euclidean dilation and stereographic projection Π:

$$\mathcal{D}(a) \equiv \Pi^{-1} \, d(a) \, \Pi \ .$$

Continuous wavelets on the sphere

- One of the first natural wavelet construction on the sphere was derived in the seminal work of Antoine and Vandergheynst (1998) (reintroduced by Wiaux 2005).
- Construct wavelet atoms from affine transformations (dilation, translation) on the sphere of a mother wavelet.
- The natural extension of translations to the sphere are rotations. Rotation of a function f on the sphere is defined by

$$[\mathcal{R}(\rho)f](\omega) = f(\rho^{-1} \cdot \omega), \quad \omega = (\theta, \varphi) \in \mathbb{S}^2, \quad \rho = (\alpha, \beta, \gamma) \in \mathrm{SO}(3) \; .$$

- How define dilation on the sphere?
- The spherical dilation operator is defined through the conjugation of the Euclidean dilation and stereographic projection Π:

$$\mathcal{D}(a) \equiv \Pi^{-1} \, d(a) \, \Pi \; .$$

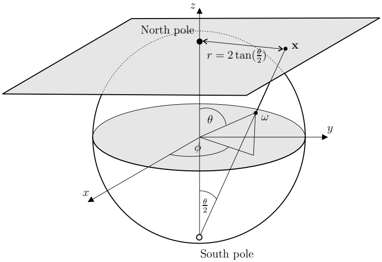

Figure: Stereographic projection.

Continuous wavelet analysis

- Wavelet family on the sphere constructed from rotations and dilations of a mother spherical wavelet Ψ:

$$\{\Psi_{a,\rho} \equiv \mathcal{R}(\rho)\mathcal{D}(a)\Psi \, : \, \rho \in \mathrm{SO}(3), \, a \in \mathbb{R}^{+}_{*}\}.$$

- The forward wavelet transform is given by

$$W^{f}_{\Psi}(a,\rho) = \langle f, \Psi_{a,\rho}\rangle = \int_{\mathbb{S}^2} \mathrm{d}\Omega(\omega)\, f(\omega)\, \Psi^{*}_{a,\rho}(\omega)\,,$$

  where $\mathrm{d}\Omega(\omega) = \sin\theta \, \mathrm{d}\theta \, \mathrm{d}\varphi$ is the usual invariant measure on the sphere.

- Wavelet coefficients (of, say, the CMB) live in $\mathrm{SO}(3) \times \mathbb{R}^{+}_{*}$; thus, directional structure is naturally incorporated.

- Fast algorithms essential (for a review see Wiaux, McEwen & Vielva 2007)
  - Factoring of rotations: McEwen *et al.* (2007), Wandelt & Gorski (2001), Risbo (1996)
  - Separation of variables: Wiaux *et al.* (2005)

- FastCSWT code available to download: http://www.jasonmcewen.org/

Continuous wavelet analysis

- Wavelet family on the sphere constructed from rotations and dilations of a mother spherical wavelet Ψ:

$$\{\Psi_{a,\rho} \equiv \mathcal{R}(\rho)\mathcal{D}(a)\Psi : \rho \in \mathrm{SO}(3),\, a \in \mathbb{R}_*^+\}.$$

- The forward wavelet transform is given by

$$W_\Psi^f(a,\rho) = \langle f, \Psi_{a,\rho}\rangle = \int_{\mathbb{S}^2} \mathrm{d}\Omega(\omega)\, f(\omega)\, \Psi_{a,\rho}^*(\omega)\ ,$$

where $\mathrm{d}\Omega(\omega) = \sin\theta\, \mathrm{d}\theta\, \mathrm{d}\varphi$ is the usual invariant measure on the sphere.

- Wavelet coefficients (of, say, the CMB) live in $\mathrm{SO}(3) \times \mathbb{R}_*^+$; thus, directional structure is naturally incorporated.

- Fast algorithms essential (for a review see Wiaux, McEwen & Vielva 2007)
  - Factoring of rotations: McEwen *et al.* (2007), Wandelt & Gorski (2001), Risbo (1996)
  - Separation of variables: Wiaux *et al.* (2005)

- FastCSWT code available to download: `http://www.jasonmcewen.org/`

Continuous wavelet analysis

- Wavelet family on the sphere constructed from rotations and dilations of a mother spherical wavelet Ψ:

$$\{\Psi_{a,\rho} \equiv \mathcal{R}(\rho)\mathcal{D}(a)\Psi \, : \, \rho \in \mathrm{SO}(3),\, a \in \mathbb{R}_*^+\}.$$

- The forward wavelet transform is given by

$$W_\Psi^f(a,\rho) = \langle f, \Psi_{a,\rho} \rangle = \int_{\mathbb{S}^2} \mathrm{d}\Omega(\omega)\, f(\omega)\, \Psi_{a,\rho}^*(\omega)\ ,$$

where $\mathrm{d}\Omega(\omega) = \sin\theta \, \mathrm{d}\theta \, \mathrm{d}\varphi$ is the usual invariant measure on the sphere.

- Wavelet coefficients (of, say, the CMB) live in $\mathrm{SO}(3) \times \mathbb{R}_*^+$; thus, directional structure is naturally incorporated.

- Fast algorithms essential (for a review see Wiaux, McEwen & Vielva 2007)
  - Factoring of rotations: McEwen *et al.* (2007), Wandelt & Gorski (2001), Risbo (1996)
  - Separation of variables: Wiaux *et al.* (2005)

- FastCSWT code available to download: `http://www.jasonmcewen.org/`

Continuous wavelet analysis

- Wavelet family on the sphere constructed from rotations and dilations of a mother spherical wavelet Ψ:
$$\{\Psi_{a,\rho} \equiv \mathcal{R}(\rho)\mathcal{D}(a)\Psi \,:\, \rho \in \mathrm{SO}(3),\, a \in \mathbb{R}_*^+\}.$$

- The forward wavelet transform is given by
$$W_\Psi^f(a,\rho) = \langle f, \Psi_{a,\rho} \rangle = \int_{\mathbb{S}^2} \mathrm{d}\Omega(\omega)\, f(\omega)\, \Psi_{a,\rho}^*(\omega) \,,$$
where $\mathrm{d}\Omega(\omega) = \sin\theta \,\mathrm{d}\theta \,\mathrm{d}\varphi$ is the usual invariant measure on the sphere.

- Wavelet coefficients (of, say, the CMB) live in $\mathrm{SO}(3) \times \mathbb{R}_*^+$; thus, directional structure is naturally incorporated.

- Fast algorithms essential (for a review see Wiaux, McEwen & Vielva 2007)
  - Factoring of rotations: McEwen *et al.* (2007), Wandelt & Gorski (2001), Risbo (1996)
  - Separation of variables: Wiaux *et al.* (2005)

- FastCSWT code available to download: `http://www.jasonmcewen.org/`

Mother wavelets

- Correspondence principle between spherical and Euclidean wavelets: inverse stereographic projection of an *admissible* wavelet on the plane yields an *admissible* wavelet on the sphere (Wiaux *et al.* 2005).

- Mother wavelets on sphere constructed from the projection of mother Euclidean wavelets defined on the plane:

$$\Psi = \Pi^{-1} \Psi_{\mathbb{R}^2} ,$$

  where $\Psi_{\mathbb{R}^2} \in L^2(\mathbb{R}^2, d^2\boldsymbol{x})$ is an admissible wavelet in the plane.

- Directional wavelets on sphere may be naturally constructed in this setting – they are simply the projection of directional Euclidean planar wavelets on to the sphere.

Mother wavelets

- Correspondence principle between spherical and Euclidean wavelets: inverse stereographic projection of an *admissible* wavelet on the plane yields an *admissible* wavelet on the sphere (Wiaux *et al.* 2005).

- Mother wavelets on sphere constructed from the projection of mother Euclidean wavelets defined on the plane:

$$\Psi = \Pi^{-1}\Psi_{\mathbb{R}^2} \ ,$$

  where $\Psi_{\mathbb{R}^2} \in \mathrm{L}^2(\mathbb{R}^2, \, \mathrm{d}^2\boldsymbol{x})$ is an admissible wavelet in the plane.

- Directional wavelets on sphere may be naturally constructed in this setting – they are simply the projection of directional Euclidean planar wavelets on to the sphere.

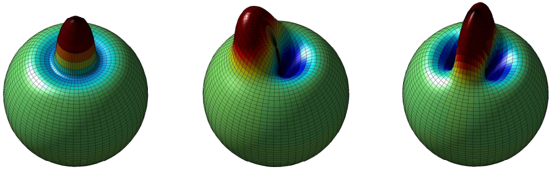

(a) SMHW (b) SBW (c) S2GDW

Figure: Spherical wavelets at scale $a, b = 0.2$.

Continuous wavelet synthesis (reconstruction)

- The inverse wavelet transform given by

$$f(\omega) = \int_0^\infty \frac{\mathrm{d}a}{a^3} \int_{\mathrm{SO}(3)} \mathrm{d}\varrho(\rho) W_\Psi^f(a,\rho)\, [\mathcal{R}(\rho)\widehat{L}_\Psi \Psi_a](\omega) \, ,$$

where $\mathrm{d}\varrho(\rho) = \sin\beta \,\mathrm{d}\alpha \,\mathrm{d}\beta \,\mathrm{d}\gamma$ is the invariant measure on the rotation group $\mathrm{SO}(3)$.

- Perfect reconstruction is ensured provided wavelets satisfy the admissibility property:

$$0 < \widehat{C}_\Psi^\ell \equiv \frac{8\pi^2}{2\ell+1} \sum_{m=-\ell}^{\ell} \int_0^\infty \frac{\mathrm{d}a}{a^3} \mid (\Psi_a)_{\ell m} \mid^2 < \infty, \quad \forall \ell \in \mathbb{N}$$

where $(\Psi_a)_{\ell m}$ are the spherical harmonic coefficients of $\Psi_a(\omega)$.

- Continuous wavelets used in many cosmological studies, for example:
  - Non-Gaussianity (*e.g.* Vielva *et al.* 2004; McEwen *et al.* 2005, 2006, 2008)
  - ISW (*e.g.* Vielva *et al.* 2005, McEwen *et al.* 2007, 2008)

- BUT...

Continuous wavelet synthesis (reconstruction)

- The inverse wavelet transform given by

$$f(\omega) = \int_0^\infty \frac{\mathrm{d}a}{a^3} \int_{\mathrm{SO}(3)} \mathrm{d}\varrho(\rho) W_\Psi^f(a, \rho) \, [\mathcal{R}(\rho)\widehat{L}_\Psi \Psi_a](\omega) \; ,$$

where $\mathrm{d}\varrho(\rho) = \sin\beta \, \mathrm{d}\alpha \, \mathrm{d}\beta \, \mathrm{d}\gamma$ is the invariant measure on the rotation group $\mathrm{SO}(3)$.

- Perfect reconstruction is ensured provided wavelets satisfy the admissibility property:

$$0 < \widehat{C}_\Psi^\ell \equiv \frac{8\pi^2}{2\ell+1} \sum_{m=-\ell}^{\ell} \int_0^\infty \frac{\mathrm{d}a}{a^3} \mid (\Psi_a)_{\ell m} \mid^2 < \infty, \quad \forall \ell \in \mathbb{N}$$

where $(\Psi_a)_{\ell m}$ are the spherical harmonic coefficients of $\Psi_a(\omega)$.

- Continuous wavelets used in many cosmological studies, for example:
  - Non-Gaussianity (*e.g.* Vielva *et al.* 2004; McEwen *et al.* 2005, 2006, 2008)
  - ISW (*e.g.* Vielva *et al.* 2005, McEwen *et al.* 2007, 2008)

- BUT...

Continuous wavelet synthesis (reconstruction)

- The inverse wavelet transform given by

$$f(\omega) = \int_0^\infty \frac{\mathrm{d}a}{a^3} \int_{\mathrm{SO}(3)} \mathrm{d}\varrho(\rho) W_\Psi^f(a, \rho) \, [\mathcal{R}(\rho) \widehat{L}_\Psi \Psi_a](\omega) \ ,$$

where $\mathrm{d}\varrho(\rho) = \sin\beta \, \mathrm{d}\alpha \, \mathrm{d}\beta \, \mathrm{d}\gamma$ is the invariant measure on the rotation group $\mathrm{SO}(3)$.

- Perfect reconstruction is ensured provided wavelets satisfy the admissibility property:

$$0 < \widehat{C}_\Psi^\ell \equiv \frac{8\pi^2}{2\ell+1} \sum_{m=-\ell}^{\ell} \int_0^\infty \frac{\mathrm{d}a}{a^3} \mid (\Psi_a)_{\ell m} \mid^2 < \infty, \quad \forall \ell \in \mathbb{N}$$

where $(\Psi_a)_{\ell m}$ are the spherical harmonic coefficients of $\Psi_a(\omega)$.

- Continuous wavelets used in many cosmological studies, for example:
  - Non-Gaussianity (*e.g.* Vielva *et al.* 2004; McEwen *et al.* 2005, 2006, 2008)
  - ISW (*e.g.* Vielva *et al.* 2005, McEwen *et al.* 2007, 2008)

- BUT...

Continuous wavelet synthesis (reconstruction)

- The inverse wavelet transform given by

$$f(\omega) = \int_0^\infty \frac{da}{a^3} \int_{SO(3)} d\varrho(\rho) W_\Psi^f(a, \rho) \, [\mathcal{R}(\rho)\widehat{L}_\Psi \Psi_a](\omega) \, ,$$

where $d\varrho(\rho) = \sin\beta \, d\alpha \, d\beta \, d\gamma$ is the invariant measure on the rotation group $SO(3)$.

- Perfect reconstruction is ensured provided wavelets satisfy the admissibility property:

$$0 < \widehat{C}_\Psi^\ell \equiv \frac{8\pi^2}{2\ell+1} \sum_{m=-\ell}^{\ell} \int_0^\infty \frac{da}{a^3} \mid (\Psi_a)_{\ell m} \mid^2 < \infty, \quad \forall \ell \in \mathbb{N}$$

where $(\Psi_a)_{\ell m}$ are the spherical harmonic coefficients of $\Psi_a(\omega)$.

- Continuous wavelets used in many cosmological studies, for example:
  - Non-Gaussianity (*e.g.* Vielva *et al.* 2004; McEwen *et al.* 2005, 2006, 2008)
  - ISW (*e.g.* Vielva *et al.* 2005, McEwen *et al.* 2007, 2008)

- BUT... **exact reconstruction not feasible in practice!**

Continuous wavelets on the sphere via harmonic dilation

- Define dilation by scaling in harmonic space (McEwen *et al.* 2006):

$$\Psi_{\ell m}(a) = \sqrt{\frac{2\ell+1}{8\pi^2}}\, \Upsilon_m(\ell a) \ ,$$

- Wavelet analysis and synthesis defined in the same manner as stereographic wavelets.
- Admissibility condition defined on the wavelet generating functions Υ

$$0 < C_\Upsilon^\ell = \sum_{m=-\ell}^{\ell} \int_0^\infty \frac{\mathrm{d}q}{q} \left|\Upsilon_m(q)\right|^2 < \infty \ .$$

- Define admissible wavelet in harmonic space:

$$\Upsilon_m(\ell a) = \mathrm{e}^{-\frac{(\ell a - L)^2 + (m-M)^2}{2}} - \mathrm{e}^{-\frac{(\ell a)^2 + L^2 + (m-M)^2}{2}} \ .$$

Continuous wavelets on the sphere via harmonic dilation

- Define dilation by scaling in harmonic space (McEwen *et al.* 2006):

$$\Psi_{\ell m}(a) = \sqrt{\frac{2\ell+1}{8\pi^2}}\, \Upsilon_m(\ell a) \ ,$$

- Wavelet analysis and synthesis defined in the same manner as stereographic wavelets.
- Admissibility condition defined on the wavelet generating functions Υ

$$0 < C_\Upsilon^\ell = \sum_{m=-\ell}^{\ell} \int_0^\infty \frac{\mathrm{d}q}{q} \left|\Upsilon_m(q)\right|^2 < \infty \ .$$

- Define admissible wavelet in harmonic space:

$$\Upsilon_m(\ell a) = \mathrm{e}^{-\frac{(\ell a - L)^2 + (m-M)^2}{2}} - \mathrm{e}^{-\frac{(\ell a)^2 + L^2 + (m-M)^2}{2}} \ .$$

Continuous wavelets on the sphere via harmonic dilation

- Define dilation by scaling in harmonic space (McEwen *et al.* 2006):

$$\Psi_{\ell m}(a) = \sqrt{\frac{2\ell+1}{8\pi^2}}\,\Upsilon_m(\ell a)\ ,$$

- Wavelet analysis and synthesis defined in the same manner as stereographic wavelets.
- Admissibility condition defined on the wavelet generating functions Υ

$$0 < C_\Upsilon^\ell = \sum_{m=-\ell}^{\ell} \int_0^\infty \frac{\mathrm{d}q}{q}\, |\Upsilon_m(q)|^2 < \infty\ .$$

- Define admissible wavelet in harmonic space:

$$\Upsilon_m(\ell a) = \mathrm{e}^{-\frac{(\ell a - L)^2 + (m-M)^2}{2}} - \mathrm{e}^{-\frac{(\ell a)^2 + L^2 + (m-M)^2}{2}}\ .$$

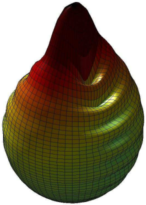

Figure: Harmonic-dilation Morlet wavelet.

Scale-discretised wavelets on the sphere

- **Exact reconstruction not feasible in practice with continuous wavelets!**
- Wiaux, McEwen, Vandergheynst, Blanc (2008)
  Exact reconstruction with directional wavelets on the sphere
- Alternatives: isotropic wavelets, pyramidal wavelets, ridgelets, curvelets (Starck *et al.* 2006); needlets (Narcowich *et al.* 2006, Baldi *et al.* 2009, Marinucci *et al.* 2008)

- Dilation performed in harmonic space.
  Following McEwen *et al.* (2006), Sanz *et al.* (2006).

- The scale-discretised wavelet $\Psi \in L^2(S^2, d\Omega)$ is defined in harmonic space:

$$\Psi_{\ell m} = \tilde{K}_\Psi(\ell) S^\Psi_{\ell m} \ .$$

- Construct wavelets to satisfy a resolution of the identity for $0 \leq \ell < L$:

$$\tilde{\Phi}^2_\Psi(\alpha^J \ell) + \sum_{j=0}^{J} \tilde{K}^2_\Psi(\alpha^j \ell) = 1 \ .$$

Scale-discretised wavelets on the sphere

- **Exact reconstruction not feasible in practice with continuous wavelets!**
- Wiaux, McEwen, Vandergheynst, Blanc (2008)
  Exact reconstruction with directional wavelets on the sphere
- Alternatives: isotropic wavelets, pyramidal wavelets, ridgelets, curvelets (Starck *et al.* 2006); needlets (Narcowich *et al.* 2006, Baldi *et al.* 2009, Marinucci *et al.* 2008)

- Dilation performed in harmonic space.
  Following McEwen *et al.* (2006), Sanz *et al.* (2006).
- The scale-discretised wavelet $\Psi \in \mathrm{L}^2(\mathrm{S}^2, \mathrm{d}\Omega)$ is defined in harmonic space:

$$\Psi_{\ell m} = \tilde{K}_\Psi(\ell) S^\Psi_{\ell m} \, .$$

- Construct wavelets to satisfy a resolution of the identity for $0 \leq \ell < L$:

$$\tilde{\Phi}^2_\Psi(\alpha^J \ell) + \sum_{j=0}^{J} \tilde{K}^2_\Psi(\alpha^j \ell) = 1 \, .$$

Scale-discretised wavelets on the sphere

- **Exact reconstruction not feasible in practice with continuous wavelets!**
- Wiaux, McEwen, Vandergheynst, Blanc (2008)
  Exact reconstruction with directional wavelets on the sphere
- Alternatives: isotropic wavelets, pyramidal wavelets, ridgelets, curvelets (Starck *et al.* 2006); needlets (Narcowich *et al.* 2006, Baldi *et al.* 2009, Marinucci *et al.* 2008)

- Dilation performed in harmonic space.
  Following McEwen *et al.* (2006), Sanz *et al.* (2006).
- The scale-discretised wavelet $\Psi \in \mathrm{L}^2(\mathrm{S}^2, \mathrm{d}\Omega)$ is defined in harmonic space:

$$\Psi_{\ell m} = \tilde{K}_\Psi(\ell) S^\Psi_{\ell m} \,.$$

- Construct wavelets to satisfy a resolution of the identity for $0 \leq \ell < L$:

$$\tilde{\Phi}^2_\Psi(\alpha^J \ell) + \sum_{j=0}^{J} \tilde{K}^2_\Psi(\alpha^j \ell) = 1 \,.$$

Scale-discretised wavelets on the sphere

- **Exact reconstruction not feasible in practice with continuous wavelets!**
- Wiaux, McEwen, Vandergheynst, Blanc (2008)
  Exact reconstruction with directional wavelets on the sphere
- Alternatives: isotropic wavelets, pyramidal wavelets, ridgelets, curvelets (Starck *et al.* 2006); needlets (Narcowich *et al.* 2006, Baldi *et al.* 2009, Marinucci *et al.* 2008)

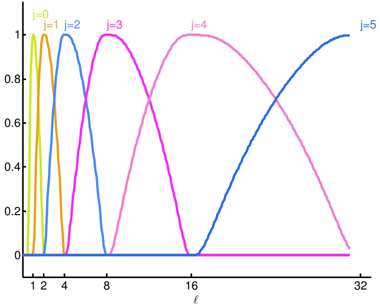

Figure: Harmonic tiling on the sphere.

- Dilation performed in harmonic space.
  Following McEwen *et al.* (2006), Sanz *et al.* (2006).
- The scale-discretised wavelet $\Psi \in \mathrm{L}^2(\mathrm{S}^2, \mathrm{d}\Omega)$ is defined in harmonic space:

$$\Psi_{\ell m} = \tilde{K}_\Psi(\ell) S^\Psi_{\ell m} \ .$$

- Construct wavelets to satisfy a resolution of the identity for $0 \leq \ell < L$:

$$\tilde{\Phi}^2_\Psi(\alpha^J \ell) + \sum_{j=0}^{J} \tilde{K}^2_\Psi(\alpha^j \ell) = 1 .$$

Scale-discretised wavelets on the sphere

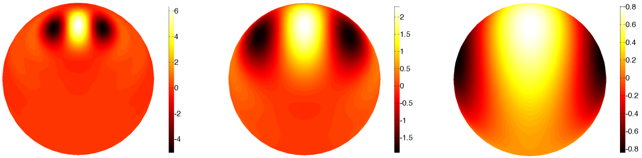

Figure: Spherical scale-discretised wavelets.

- The scale-discretised wavelet transform is given by the usual projection onto each wavelet:

$$W^f_{\Psi}(\rho, \alpha^j) = \langle f, \Psi_{\rho,\alpha^j} \rangle = \int_{\mathbb{S}^2} \mathrm{d}\Omega(\omega)\, f(\omega)\, \Psi^*_{\rho,\alpha^j}(\omega) \ .$$

- The original function may be recovered exactly in practice from the wavelet (and scaling) coefficients:

$$f(\omega) = \left[\Phi_{\alpha^J} f\right](\omega) + \sum_{j=0}^{J} \int_{\mathrm{SO}(3)} \mathrm{d}\varrho(\rho)\, W^f_{\Psi}\left(\rho, \alpha^j\right) \left[R(\rho)\, L^{\mathrm{d}} \Psi_{\alpha^j}\right](\omega) \ .$$

Scale-discretised wavelets on the sphere

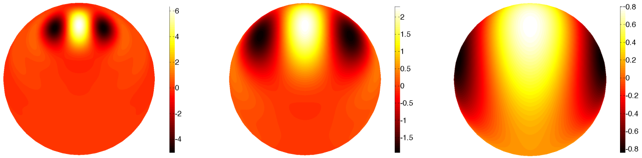

Figure: Spherical scale-discretised wavelets.

- The scale-discretised wavelet transform is given by the usual projection onto each wavelet:

$$W^f_\Psi(\rho, \alpha^j) = \langle f, \Psi_{\rho,\alpha^j} \rangle = \int_{\mathbb{S}^2} \mathrm{d}\Omega(\omega)\, f(\omega)\, \Psi^*_{\rho,\alpha^j}(\omega)\,.$$

- The original function may be recovered exactly in practice from the wavelet (and scaling) coefficients:

$$f(\omega) = [\Phi_{\alpha^J} f](\omega) + \sum_{j=0}^{J} \int_{\mathrm{SO}(3)} \mathrm{d}\varrho(\rho)\, W^f_\Psi(\rho, \alpha^j) \left[R(\rho)\, L^{\mathrm{d}} \Psi_{\alpha^j} \right](\omega)\,.$$

Scale-discretised wavelets on the sphere

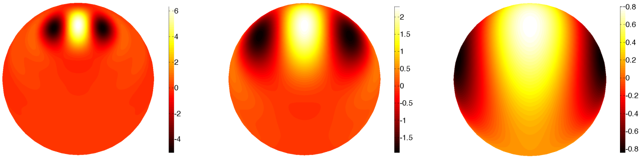

Figure: Spherical scale-discretised wavelets.

- The scale-discretised wavelet transform is given by the usual projection onto each wavelet:

$$W^f_\Psi(\rho, \alpha^j) = \langle f, \Psi_{\rho,\alpha^j} \rangle = \int_{\mathbb{S}^2} \mathrm{d}\Omega(\omega) \, f(\omega) \, \Psi^*_{\rho,\alpha^j}(\omega) \; .$$

- The original function may be recovered exactly in practice from the wavelet (and scaling) coefficients:

$$f(\omega) = [\Phi_{\alpha^J} f](\omega) + \sum_{j=0}^{J} \int_{\mathrm{SO}(3)} \mathrm{d}\varrho(\rho) \, W^f_\Psi\left(\rho, \alpha^j\right) \left[R(\rho) \, L^{\mathrm{d}} \Psi_{\alpha^j}\right](\omega) \; .$$

Steerability

- The scale-discretised wavelet $\Psi \in \mathrm{L}^2(\mathbb{S}^2, \mathrm{d}\Omega)$ is defined in harmonic space in factorised form:

$$\Psi_{\ell m} = \tilde{K}_\Psi(\ell) S^\Psi_{\ell m} \ .$$

- Without loss of generality, impose

$$\sum_m |S^\Psi_{\ell m}|^2 = 1 \ ,$$

such that localisation governed largely by $\tilde{K}_\Psi(\ell)$ and directionality by $S^\Psi_{\ell m}$.

- By imposing an azimuthal band-limit N, *i.e.* $S^\Psi_{\ell m} = 0, \ \forall m \geq N$, we recover steerable wavelets that satisfy

$$(\mathcal{R}^z(\chi)\Psi)(\omega) = \sum_{p=0}^{2N-2} k(\chi - \chi_p) \ (\mathcal{R}^z(\chi_p)\Psi)(\omega) \ .$$

- By the linearity of the wavelet transform, property extends to wavelet coefficients.

Steerability

- The scale-discretised wavelet $\Psi \in \mathrm{L}^2(\mathbb{S}^2, \mathrm{d}\Omega)$ is defined in harmonic space in factorised form:

$$\Psi_{\ell m} = \tilde{K}_\Psi(\ell) S^\Psi_{\ell m} \ .$$

- Without loss of generality, impose

$$\sum_m |S^\Psi_{\ell m}|^2 = 1 \ ,$$

such that localisation governed largely by $\tilde{K}_\Psi(\ell)$ and directionality by $S^\Psi_{\ell m}$.

- By imposing an azimuthal band-limit N, *i.e.* $S^\Psi_{\ell m} = 0, \ \forall m \geq N$, we recover steerable wavelets that satisfy

$$\big(\mathcal{R}^z(\chi)\Psi\big)(\omega) = \sum_{p=0}^{2N-2} k(\chi - \chi_p) \ \big(\mathcal{R}^z(\chi_p)\Psi\big)(\omega) \ .$$

- By the linearity of the wavelet transform, property extends to wavelet coefficients.

Steerability

- The scale-discretised wavelet $\Psi \in \mathrm{L}^2(\mathrm{S}^2, \mathrm{d}\Omega)$ is defined in harmonic space in factorised form:

$$\Psi_{\ell m} = \tilde{K}_\Psi(\ell) S^\Psi_{\ell m} \, .$$

- Without loss of generality, impose

$$\sum_m |S^\Psi_{\ell m}|^2 = 1 \, ,$$

  such that localisation governed largely by $\tilde{K}_\Psi(\ell)$ and directionality by $S^\Psi_{\ell m}$.

- By imposing an azimuthal band-limit N, *i.e.* $S^\Psi_{\ell m} = 0, \ \forall m \geq N$, we recover steerable wavelets that satisfy

$$\big(\mathcal{R}^z(\chi)\Psi\big)(\omega) = \sum_{p=0}^{2N-2} k(\chi - \chi_p) \, \big(\mathcal{R}^z(\chi_p)\Psi\big)(\omega) \, .$$

- By the linearity of the wavelet transform, property extends to wavelet coefficients.

Fast algorithms

- Wavelet analysis can be posed as an inverse Wigner transform on $\mathrm{SO}(3)$:

$$W^f_{\Psi^j}(\rho) = \langle f, \Psi^j_\rho \rangle = \sum_{\ell m n} \frac{2\ell+1}{8\pi^2} \left(W^f_{\Psi^j}\right)^\ell_{mn} D^{\ell *}_{mn}(\rho) \; ,$$

  where

$$\left(W^f_{\Psi^j}\right)^\ell_{mn} = \frac{8\pi^2}{2\ell+1} f_{\ell m} \Psi^{j*}_{\ell n} \; ,$$

  which can be computed efficiently via a factoring of rotations (Risbo 1996, Wandelt & Gorski 2001).

- Wavelet synthesis can be posed as an forward Wigner transform on $\mathrm{SO}(3)$:

$$f_{\ell m} = \sum_{jn} \frac{2\ell+1}{8\pi^2} \left(W^f_{\Psi^j}\right)^\ell_{mn} \Psi^j_{\ell n} \; ,$$

  where

$$\left(W^f_{\Psi^j}\right)^\ell_{mn} = \int_{\mathrm{SO}(3)} \mathrm{d}\varrho(\rho) \; W^f_{\Psi^j}(\rho) D^\ell_{mn}(\rho) \; ,$$

  which can be computed efficiently via a factoring of rotations (Risbo 1996) and exactly by employing the Driscoll & Healy (1994) sampling theorem.

Fast algorithms

- Wavelet analysis can be posed as an inverse Wigner transform on $\mathrm{SO}(3)$:

$$W^{f}_{\Psi^j}(\rho) = \langle f, \Psi^j_\rho \rangle = \sum_{\ell m n} \frac{2\ell+1}{8\pi^2} (W^{f}_{\Psi^j})^{\ell}_{mn} D^{\ell *}_{mn}(\rho) \ ,$$

  where

$$(W^{f}_{\Psi^j})^{\ell}_{mn} = \frac{8\pi^2}{2\ell+1} f_{\ell m} \Psi^{j*}_{\ell n} \ ,$$

  which can be computed efficiently via a factoring of rotations (Risbo 1996, Wandelt & Gorski 2001).

- Wavelet synthesis can be posed as an forward Wigner transform on $\mathrm{SO}(3)$:

$$f_{\ell m} = \sum_{jn} \frac{2\ell+1}{8\pi^2} (W^{f}_{\Psi^j})^{\ell}_{mn} \Psi^{j}_{\ell n} \ ,$$

  where

$$(W^{f}_{\Psi^j})^{\ell}_{mn} = \int_{\mathrm{SO}(3)} \mathrm{d}\varrho(\rho) \ W^{f}_{\Psi^j}(\rho) D^{\ell}_{mn}(\rho) \ ,$$

  which can be computed efficiently via a factoring of rotations (Risbo 1996) and exactly by employing the Driscoll & Healy (1994) sampling theorem.

Driscoll & Healy (DH) sampling theorem

- Canonical sampling theorem on the sphere derived by Driscoll & Healy (1994).

$\Rightarrow$ $N_{\mathrm{DH}} = (2L-1)2L + 1 \sim 4L^2$ samples on the sphere.

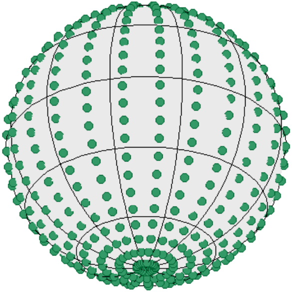

Figure: Sample positions of the DH sampling theorem.

McEwen & Wiaux (MW) sampling theorem

- A new sampling theorem on the sphere (McEwen & Wiaux 2011).

  $\Rightarrow$ $N_{\rm MW} = (L-1)(2L-1)+1 \sim 2L^2$ samples on the sphere.

- Reduced the Nyquist rate on the sphere by a factor of two.

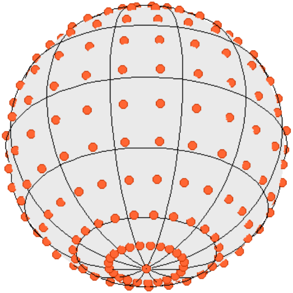

Figure: Sample positions of the MW sampling theorem.

Codes to compute harmonic transforms

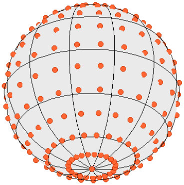

SSHT code: Spin spherical harmonic transforms

A novel sampling theorem on the sphere

McEwen & Wiaux (2011)

All codes available from: `http://www.jasonmcewen.org/`

Codes to compute scale-discretised wavelets on the sphere

S2DW code

Exact reconstruction with directional wavelets on the sphere
Wiaux, McEwen, Vandergheynst, Blanc (2008)

- Fortran
- Parallelised
- Supports directional, steerable wavelets

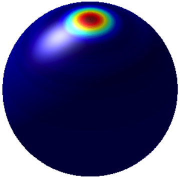

S2LET code

S2LET: A code to perform fast wavelet analysis on the sphere
Leistedt, McEwen, Vandergheynst, Wiaux (2012)

- C, Matlab, IDL, Java
- Support only axisymmetric wavelets at present
- Future extensions:
  - Directional, steerable wavelets
  - Faster algorithms to perform wavelet transforms
  - Spin wavelets

All codes available from: `http://www.jasonmcewen.org/`

Scale-discretised wavelets on the sphere

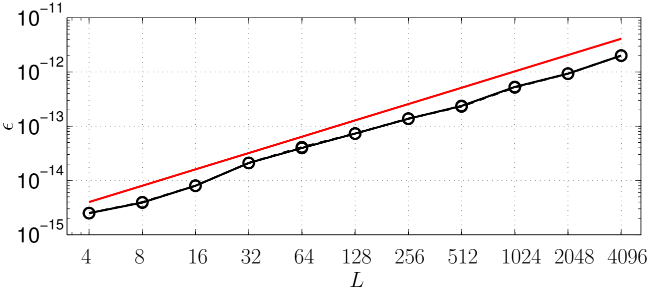

Figure: Computation time of the scale-discretised wavelet transform.

Scale-discretised wavelets on the sphere

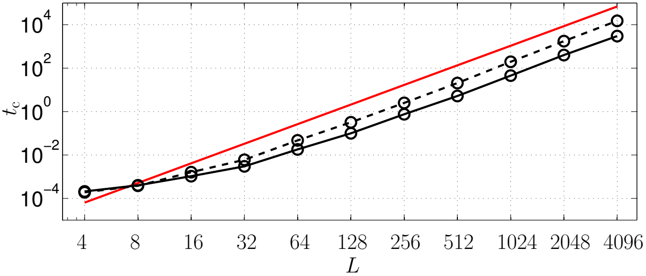

Figure: Numerical accuracy of the scale-discretised wavelet transform.

Scale-discretised wavelet transform of the Earth

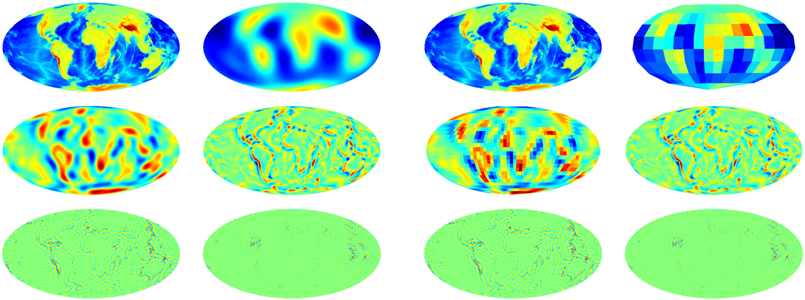

(a) Undecimated (b) Multi-resolution

Figure: Scale-discretised wavelet transform of a topography map of the Earth.

Outline

Galaxy surveys

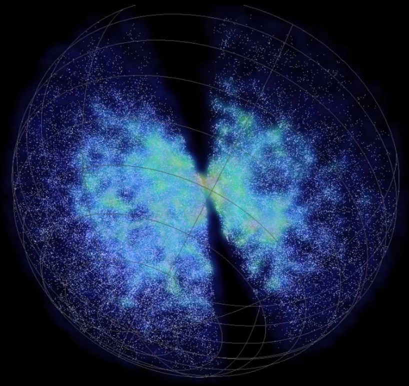

Credit: SDSS

Fourier-Laguerre transform on the ball

- Fourier-Bessel functions are the canonical orthogonal basis on the sphere → but do not admit a sampling theorem.
- Developed a Fourier-Laguerre transform and corresponding sampling theorem on the ball (Leistedt & McEwen 2012).
- Define the radial basis functions by

$$K_p(r) \equiv \sqrt{\frac{p!}{(p+2)!}} \frac{e^{-r/2\tau}}{\sqrt{\tau^3}} L_p^{(2)}\left(\frac{r}{\tau}\right) ,$$

  where $L_p^{(2)}$ is the p-th generalised Laguerre polynomial of order two.
- Define the Fourier-Laguerre basis functions by $Z_{\ell mp}(\boldsymbol{r}) = K_p(r) Y_{\ell m}(\omega)$.

Fourier-Laguerre transform on the ball

- Fourier-Bessel functions are the canonical orthogonal basis on the sphere → but do not admit a sampling theorem.
- Developed a Fourier-Laguerre transform and corresponding sampling theorem on the ball (Leistedt & McEwen 2012).
- Define the radial basis functions by

$$K_p(r) \equiv \sqrt{\frac{p!}{(p+2)!}} \frac{e^{-r/2\tau}}{\sqrt{\tau^3}} L_p^{(2)}\left(\frac{r}{\tau}\right) ,$$

  where $L_p^{(2)}$ is the p-th generalised Laguerre polynomial of order two.
- Define the Fourier-Laguerre basis functions by $Z_{\ell mp}(\boldsymbol{r}) = K_p(r) Y_{\ell m}(\omega)$.

Fourier-Laguerre transform on the ball

- Fourier-Bessel functions are the canonical orthogonal basis on the sphere $\rightarrow$ but do not admit a sampling theorem.
- Developed a Fourier-Laguerre transform and corresponding sampling theorem on the ball (Leistedt & McEwen 2012).
- Define the radial basis functions by

$$K_p(r) \equiv \sqrt{\frac{p!}{(p+2)!}} \frac{e^{-r/2\tau}}{\sqrt{\tau^3}} L_p^{(2)}\left(\frac{r}{\tau}\right) ,$$

where $L_p^{(2)}$ is the p-th generalised Laguerre polynomial of order two.

- Define the Fourier-Laguerre basis functions by $Z_{\ell m p}(\boldsymbol{r}) = K_p(r) Y_{\ell m}(\omega)$.

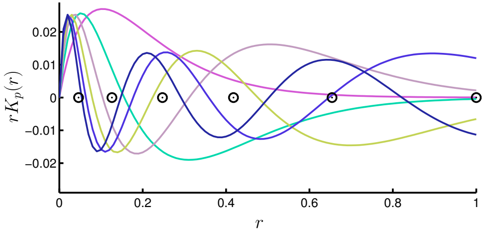

Fourier-Laguerre transform on the ball

- For a band-limited signal, we can compute the Fourier-Laguerre transform exactly.
- Compute Fourier-Bessel coefficients exactly from Fourier-Laguerre coefficients.

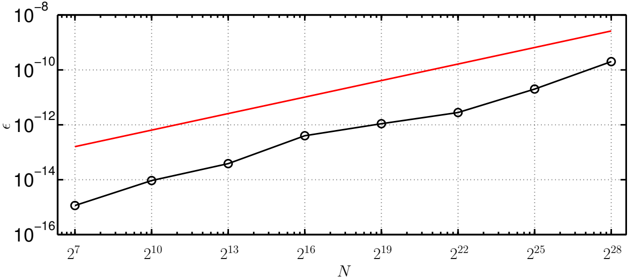

Figure: Numerical accuracy of Fourier-Laguerre transform

Fourier-Laguerre transform on the ball

- Fast algorithms to compute the Fourier-Laguerre transform.

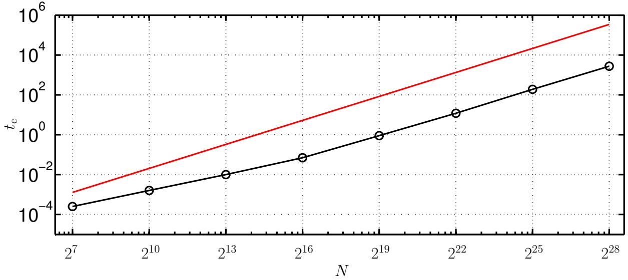

Figure: Computation time of Fourier-Laguerre transform

Codes to compute harmonic transforms

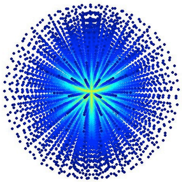

FLAG code: Fourier-Laguerre transforms
Exact wavelets on the ball
Leistedt & McEwen (2012)

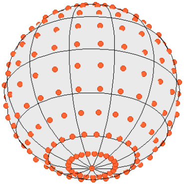

SSHT code: Spin spherical harmonic transforms
A novel sampling theorem on the sphere
McEwen & Wiaux (2011)

All codes available from: `http://www.jasonmcewen.org/`

Fourier-Laguerre translation and convolution

- We construct translation and convolution operators on the radial line by analogy with the infinite line.
- For the standard orthogonal basis $\phi_\omega(x) = \mathrm{e}^{\mathrm{i}\omega x}$ translation of the basis functions defined by the shift of coordinates:

$$(\mathcal{T}_u^{\mathbb{R}}\phi_\omega)(x) \equiv \phi_\omega(x-u) = \phi_\omega^*(u)\phi_\omega(x) \ .$$

- Define translation of the spherical Laguerre basis functions on the radial line by analogy:

$$(\mathcal{T}_s K_p)(r) \equiv K_p(s) K_p(r) \ .$$

- Define convolution on the radial line of by

$$(f \star h)(r) \equiv \langle f | \mathcal{T}_r h \rangle = \int_{\mathbb{R}+} \mathrm{d}s s^2 f(s) \left(\mathcal{T}_r h\right)(s),$$

from which it follows that radial convolution in harmonic space is given by the product

$$(f \star h)_p = \langle f \star h | K_p \rangle = f_p h_p \ .$$

Fourier-Laguerre translation and convolution

- We construct translation and convolution operators on the radial line by analogy with the infinite line.

- For the standard orthogonal basis $\phi_\omega(x) = e^{i\omega x}$ translation of the basis functions defined by the shift of coordinates:

$$(\mathcal{T}_u^{\mathbb{R}} \phi_\omega)(x) \equiv \phi_\omega(x-u) = \phi_\omega^*(u)\phi_\omega(x) \ .$$

- Define translation of the spherical Laguerre basis functions on the radial line by analogy:

$$(\mathcal{T}_s K_p)(r) \equiv K_p(s) K_p(r) \ .$$

- Define convolution on the radial line of by

$$(f \star h)(r) \equiv \langle f | \mathcal{T}_r h \rangle = \int_{\mathbb{R}^+} \mathrm{d}s s^2 f(s) \left(\mathcal{T}_r h\right)(s),$$

from which it follows that radial convolution in harmonic space is given by the product

$$(f \star h)_p = \langle f \star h | K_p \rangle = f_p h_p \ .$$

Fourier-Laguerre translation and convolution

- We construct translation and convolution operators on the radial line by analogy with the infinite line.
- For the standard orthogonal basis $\phi_\omega(x) = e^{i\omega x}$ translation of the basis functions defined by the shift of coordinates:

$$(\mathcal{T}_u^{\mathbb{R}} \phi_\omega)(x) \equiv \phi_\omega(x - u) = \phi_\omega^*(u)\phi_\omega(x) \ .$$

- Define translation of the spherical Laguerre basis functions on the radial line by analogy:

$$(\mathcal{T}_s K_p)(r) \equiv K_p(s) K_p(r) \ .$$

- Define convolution on the radial line of by

$$(f \star h)(r) \equiv \langle f | \mathcal{T}_r h \rangle = \int_{\mathbb{R}+} \mathrm{d}s s^2 f(s) \left(\mathcal{T}_r h\right)(s),$$

from which it follows that radial convolution in harmonic space is given by the product

$$(f \star h)_p = \langle f \star h | K_p \rangle = f_p h_p \ .$$

Fourier-Laguerre translation and convolution

- Translation corresponds to convolution with the Dirac delta:

$$(f \star \delta_s)(r) = \sum_{p=0}^{\infty} f_p K_p(s) K_p(r) = (\mathcal{T}_s f)(r) \ .$$

Fourier-Laguerre translation and convolution

- Translation corresponds to convolution with the Dirac delta:

$$(f \star \delta_s)(r) = \sum_{p=0}^{\infty} f_p K_p(s) K_p(r) = (\mathcal{T}_s f)(r) \ .$$

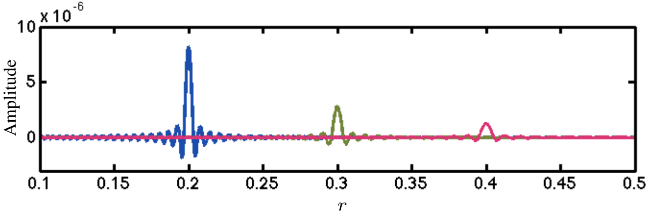

Figure: Band limited translated Dirac delta functions

Fourier-Laguerre translation and convolution

- Translation corresponds to convolution with the Dirac delta:

$$(f \star \delta_s)(r) = \sum_{p=0}^{\infty} f_p K_p(s) K_p(r) = (\mathcal{T}_s f)(r) \; .$$

- Angular aperture of localised functions (and flaglets) is invariant under radial translation.

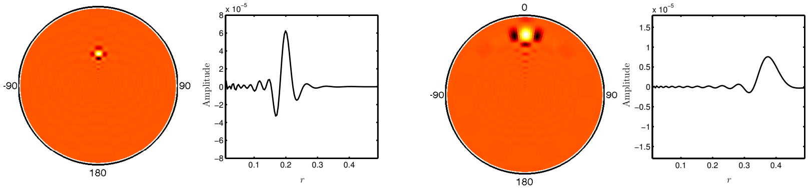

(a) Wavelet kernel translated by $r = 0.2$ (b) Wavelet kernel translated by $r = 042$

Figure: Slices of an axisymmetric flaglet wavelet kernel plotted on the ball of radius $R = 0.5$.

Fourier-Laguerre translation and convolution

- Translation corresponds to convolution with the Dirac delta:

$$(f \star \delta_s)(r) = \sum_{p=0}^{\infty} f_p K_p(s) K_p(r) = (\mathcal{T}_s f)(r) \; .$$

- Angular aperture of localised functions (and flaglets) is invariant under radial translation.

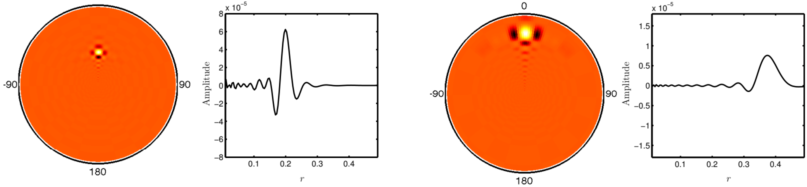

(a) Wavelet kernel translated by $r = 0.2$

(b) Wavelet kernel translated by $r = 042$

Figure: Slices of an axisymmetric flaglet wavelet kernel plotted on the ball of radius $R = 0.5$.

Scale-discretised wavelets on the ball

- *Exact wavelets on the ball* (Leistedt & McEwen 2012).
- Define translation and convolution operators on the radial line.
- Dilation performed in harmonic space.
- Scale-discretised wavelet $\Psi \in \mathrm{L}^2(B^3)$ is defined in harmonic space:

$$\Psi^{jj'}_{\ell mp} \equiv \sqrt{\frac{2\ell+1}{4\pi}}\, \kappa_\lambda\left(\frac{\ell}{\lambda^j}\right) \kappa_\nu\left(\frac{p}{\nu^{j'}}\right) \delta_{m0}\,.$$

- Construct wavelets to satisfy a resolution of the identity:

$$\frac{4\pi}{2\ell+1}\left(|\Phi_{\ell 0p}|^2 + \sum_{j=J_0}^{J} \sum_{j'=J'_0}^{J'} |\Psi^{jj'}_{\ell 0p}|^2\right) = 1,\ \forall \ell, p.$$

Scale-discretised wavelets on the ball

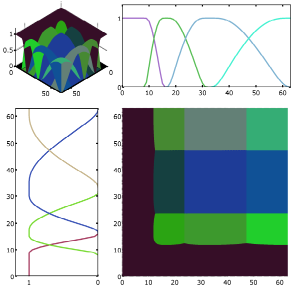

Figure: Tiling of Fourier-Laguerre space.

- *Exact wavelets on the ball* (Leistedt & McEwen 2012).
- Define translation and convolution operators on the radial line.
- Dilation performed in harmonic space.
- Scale-discretised wavelet $\Psi \in \mathrm{L}^2(B^3)$ is defined in harmonic space:

$$\Psi^{jj'}_{\ell m p} \equiv \sqrt{\frac{2\ell+1}{4\pi}}\, \kappa_\lambda\left(\frac{\ell}{\lambda^j}\right) \kappa_\nu\left(\frac{p}{\nu^{j'}}\right) \delta_{m0}\, .$$

- Construct wavelets to satisfy a resolution of the identity:

$$\frac{4\pi}{2\ell+1}\left(|\Phi_{\ell 0 p}|^2 + \sum_{j=J_0}^{J} \sum_{j'=J'_0}^{J'} |\Psi^{jj'}_{\ell 0 p}|^2 \right) = 1, \ \forall \ell, p.$$

Scale-discretised wavelets on the ball

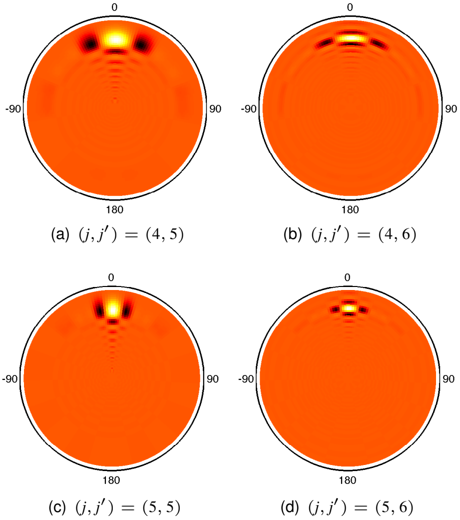

Figure: Scale-discretised wavelets on the ball.

Scale-discretised wavelets on the ball

- The scale-discretised wavelet transform is given by the usual projection onto each wavelet:

$$W^{\Psi^{jj'}}(\boldsymbol{r}) \equiv (f \star \Psi^{jj'})(\boldsymbol{r}) = \langle f | \mathcal{T}_r \mathcal{R}_\omega \Psi^{jj'} \rangle = \int_{B^3} \mathrm{d}^3\boldsymbol{r}' f(\boldsymbol{r}') (\mathcal{T}_r \mathcal{R}_\omega \Psi^{jj'})(\boldsymbol{r}') \ .$$

- The original function may be recovered exactly in practice from the wavelet (and scaling) coefficients:

$$f(\boldsymbol{r}) \quad = \quad \int_{B^3} \mathrm{d}^3\boldsymbol{r}' W^{\Phi}(\boldsymbol{r}') (\mathcal{T}_r \mathcal{R}_\omega \Phi)(\boldsymbol{r}') + \sum_{j=J_0}^{J} \sum_{j'=J_0'}^{J'} \int_{B^3} \mathrm{d}^3\boldsymbol{r}' W^{\Psi^{jj'}}(\boldsymbol{r}') (\mathcal{T}_r \mathcal{R}_\omega \Psi^{jj'})(\boldsymbol{r}') \ .$$

- Alternatives: Spherical 3D isotropic wavelets (Lanusse, Rassat & Starck 2012)

Code for scale-discretised wavelet on the ball

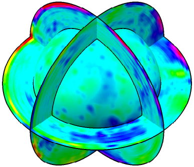

FLAGLET code

Exact wavelets on the ball

Leistedt & McEwen (2012)

- C, Matlab, IDL, Java
- Exact (Fourier-LAGuerre) wavelets on the ball – coined *flaglets*!

Available from: `http://www.jasonmcewen.org/`

Scale-discretised wavelets on the ball

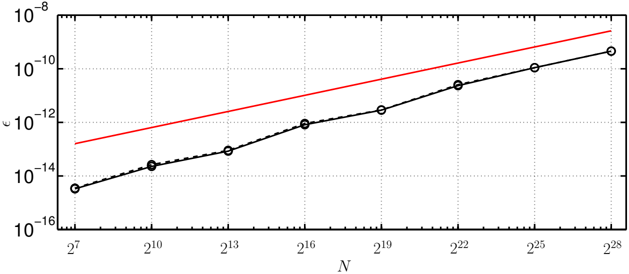

Figure: Numerical accuracy of the flaglet transform.

Scale-discretised wavelets on the ball

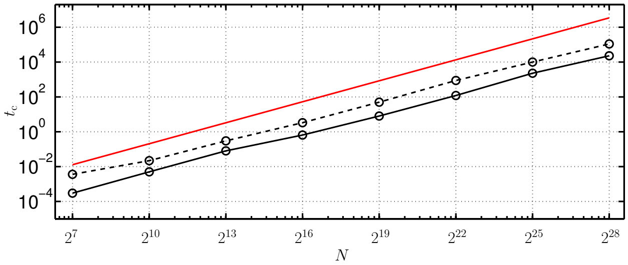

Figure: Computation time of the flaglet transform.

Scale-discretised wavelet transform of N-body simulation

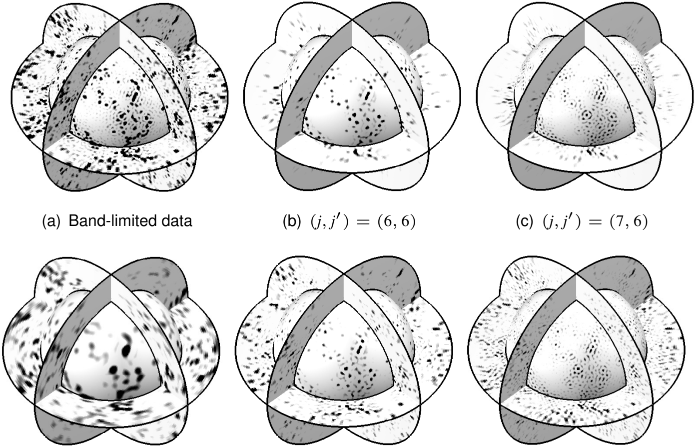

(a) Band-limited data (b) $(j, j') = (6, 6)$ (c) $(j, j') = (7, 6)$

(d) Scaling coefficients (e) $(j, j') = (6, 7)$ (f) $(j, j') = (7, 7)$

Figure: Wavelet transform of of an N-body simulation.

Scale-discretised wavelet denoising on the ball

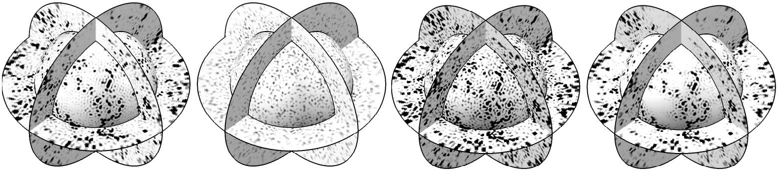

(a) Ground truth (b) Noise (c) Noisy (SNR=5dB) (d) Denoised (SNR=11dB)

Figure: Denoising of an N-body simulation.

Scale-discretised wavelet denoising on the ball

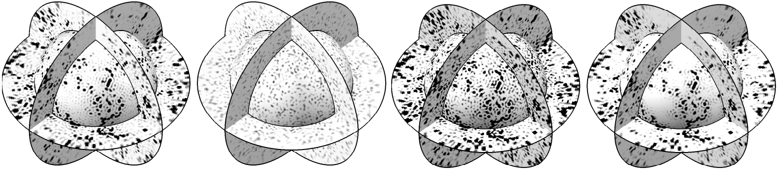

(a) Ground truth (b) Noise (c) Noisy (SNR=5dB) (d) Denoised (SNR=11dB)

Figure: Denoising of an N-body simulation.

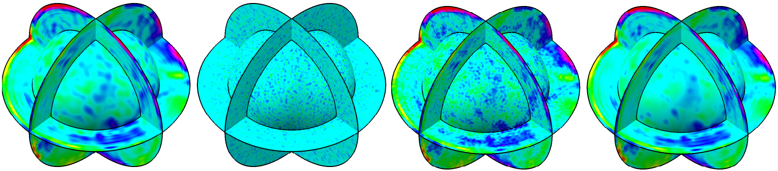

(a) Ground truth (b) Noise (c) Noisy (SNR=5dB) (d) Denoised (SNR=17dB)

Figure: Denoising of a seismological Earth model.

Outline

Cosmic structure

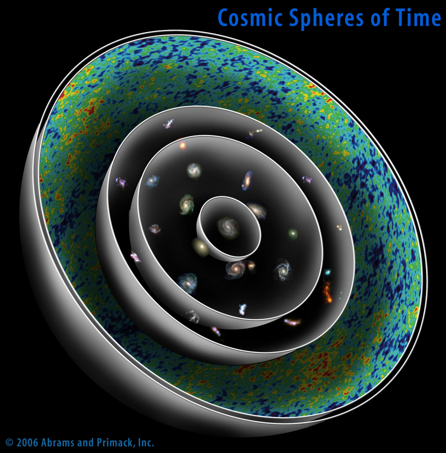

Cosmic strings

- Symmetry breaking phase transitions in the early Universe → topological defects.
- Cosmic strings well-motivated phenomenon that arise when axial or cylindrical symmetry is broken → line-like discontinuities in the fabric of the Universe.
- Although we have not yet observed cosmic strings, we have observed string-like topological defects in other media, e.g. ice and liquid crystal.
- Cosmic strings are distinct to the fundamental superstrings of string theory.
- However, recent developments in string theory suggest the existence of macroscopic superstrings that could play a similar role to cosmic strings.
- The detection of cosmic strings would open a new window into the physics of the Universe!

Figure: Optical microscope photograph of a thin film of freely suspended nematic liquid crystal after a temperature quench. [Credit: Chuang *et al.* (1991).]

Cosmic strings

- Symmetry breaking phase transitions in the early Universe → topological defects.
- Cosmic strings well-motivated phenomenon that arise when axial or cylindrical symmetry is broken → line-like discontinuities in the fabric of the Universe.
- Although we have not yet observed cosmic strings, we have observed string-like topological defects in other media, e.g. ice and liquid crystal.
- Cosmic strings are distinct to the fundamental superstrings of string theory.
- However, recent developments in string theory suggest the existence of macroscopic superstrings that could play a similar role to cosmic strings.
- The detection of cosmic strings would open a new window into the physics of the Universe!

Figure: Optical microscope photograph of a thin film of freely suspended nematic liquid crystal after a temperature quench. [Credit: Chuang *et al.* (1991).]

Cosmic strings

- Symmetry breaking phase transitions in the early Universe → topological defects.
- Cosmic strings well-motivated phenomenon that arise when axial or cylindrical symmetry is broken → line-like discontinuities in the fabric of the Universe.
- Although we have not yet observed cosmic strings, we have observed string-like topological defects in other media, e.g. ice and liquid crystal.
- Cosmic strings are distinct to the fundamental superstrings of string theory.
- However, recent developments in string theory suggest the existence of macroscopic superstrings that could play a similar role to cosmic strings.
- The detection of cosmic strings would open a new window into the physics of the Universe!

Figure: Optical microscope photograph of a thin film of freely suspended nematic liquid crystal after a temperature quench. [Credit: Chuang *et al.* (1991).]

Observational signatures of cosmic strings

- Spacetime about a cosmic string is canonical, with a three-dimensional wedge removed (Vilenkin 1981).
- Strings moving transverse to the line of sight induce line-like discontinuities in the CMB (Kaiser & Stebbins 1984).
- The amplitude of the induced contribution scales with $G\mu$, the string tension.

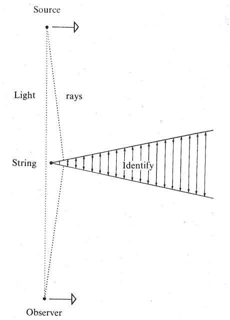

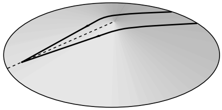

Spacetime around a cosmic string. [Credit: Kaiser & Stebbins 1984, DAMTP.]

Observational signatures of cosmic strings

- Make contact between theory and data using high-resolution simulations.
- Amplitude of the signal is given by the string tension $G\mu$.
- Search for a weak string signal s embedded in the CMB c, with observations d given by

$$d = c + s \, .$$

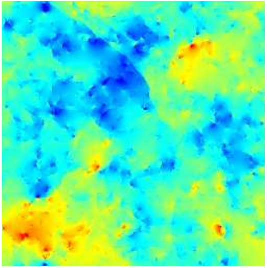

(a) Flat patch (Fraisse *et al.* 2008)

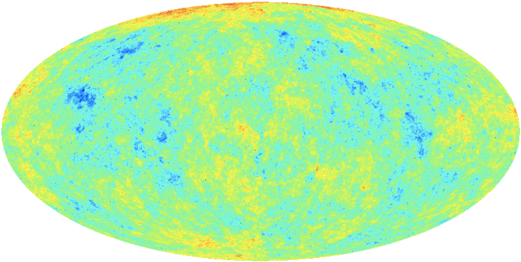

(b) Full-sky (Ringeval *et al.* 2012)

Figure: Cosmic string simulations.

Using wavelets to detect cosmic strings

- Ongoing work of McEwen, Feeney, Peiris, Wiaux, Ringeval & Bouchet.
- Adopt the scale-discretised wavelet transform on the sphere (Wiaux, McEwen *et al.* 2008), where we denote the wavelet coefficients of the data d by $W^d_{j\rho} = \langle d, \Psi_{j\rho} \rangle$ for scale $j \in \mathbb{Z}^+$ and position $\rho \in \mathrm{SO}(3)$.

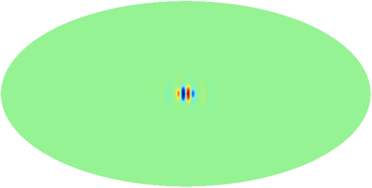

Figure: Example wavelet.

- Wavelet transform yields a sparse representation of the string signal $\rightarrow$ hope to effectively separate the CMB and string signal in wavelet space.

Using wavelets to detect cosmic strings

- Ongoing work of McEwen, Feeney, Peiris, Wiaux, Ringeval & Bouchet.
- Adopt the scale-discretised wavelet transform on the sphere (Wiaux, McEwen *et al.* 2008), where we denote the wavelet coefficients of the data d by $\boxed{W^d_{j\rho} = \langle d, \; \Psi_{j\rho} \rangle}$ for scale $j \in \mathbb{Z}^+$ and position $\rho \in \mathrm{SO}(3)$.

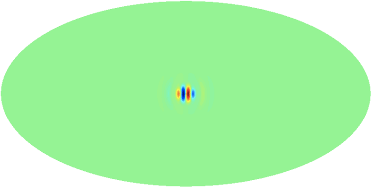

Figure: Example wavelet.

- Wavelet transform yields a sparse representation of the string signal $\rightarrow$ hope to effectively separate the CMB and string signal in wavelet space.

Using wavelets to detect cosmic strings

- Ongoing work of McEwen, Feeney, Peiris, Wiaux, Ringeval & Bouchet.
- Adopt the scale-discretised wavelet transform on the sphere (Wiaux, McEwen *et al.* 2008), where we denote the wavelet coefficients of the data d by $W^{d}_{j\rho} = \langle d, \Psi_{j\rho} \rangle$ for scale $j \in \mathbb{Z}^{+}$ and position $\rho \in \mathrm{SO}(3)$.

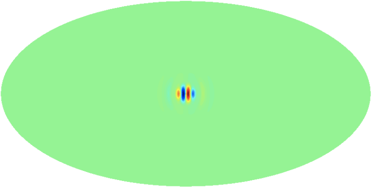

Figure: Example wavelet.

- Wavelet transform yields a sparse representation of the string signal $\rightarrow$ hope to effectively separate the CMB and string signal in wavelet space.

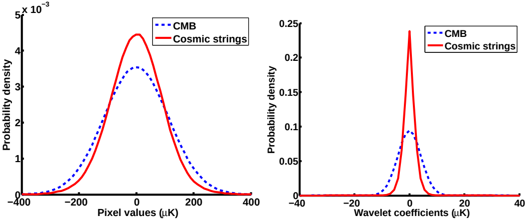

Figure: Distribution of CMB and string signal in pixel (left) and wavelet space (right).

Learning the statistics of the CMB and string signals in wavelet space

- Need to determine statistical description of the CMB and string signals in wavelet space.
- Calculate analytically the probability distribution of the CMB in wavelet space:

$$\mathrm{P}_j^c(W_{j\rho}^c) = \frac{1}{\sqrt{2\pi(\sigma_j^c)^2}} \mathrm{e}^{\left(-\frac{1}{2}\left(\frac{W_{j\rho}^c}{\sigma_j^c}\right)^2\right)} , \quad \text{where} \quad (\sigma_j^c)^2 = \langle W_{j\rho}^c \, W_{j\rho}^{c\;*} \rangle = \sum_{\ell m} C_\ell \, |(\Psi_j)_{\ell m}|^2 .$$

- Fit a generalised Gaussian distribution (GGD) for the wavelet coefficients of a string training map (*cf.* Wiaux *et al.* 2009):

$$\mathrm{P}_j^s(W_{j\rho}^s \mid G\mu) = \frac{\upsilon_j}{2G\mu\nu_j\Gamma(\upsilon_j^{-1})} \mathrm{e}^{\left(-\left|\frac{W_{j\rho}^s}{G\mu\nu_j}\right|^{\upsilon_j}\right)} ,$$

with scale parameter ν_j and shape parameter υ_j.

Learning the statistics of the CMB and string signals in wavelet space

- Need to determine statistical description of the CMB and string signals in wavelet space.
- Calculate analytically the probability distribution of the CMB in wavelet space:

$$\mathrm{P}_j^c(W_{j\rho}^c) = \frac{1}{\sqrt{2\pi(\sigma_j^c)^2}} \mathrm{e}^{\left(-\frac{1}{2}\left(\frac{W_{j\rho}^c}{\sigma_j^c}\right)^2\right)}, \quad \text{where} \quad (\sigma_j^c)^2 = \langle W_{j\rho}^c \, W_{j\rho}^{c\;*} \rangle = \sum_{\ell m} C_\ell \, |(\Psi_j)_{\ell m}|^2 .$$

- Fit a generalised Gaussian distribution (GGD) for the wavelet coefficients of a string training map (*cf.* Wiaux *et al.* 2009):

$$\mathrm{P}_j^s(W_{j\rho}^s \mid G\mu) = \frac{\upsilon_j}{2G\mu\nu_j\Gamma(\upsilon_j^{-1})} \mathrm{e}^{\left(-\left|\frac{W_{j\rho}^s}{G\mu\nu_j}\right|^{\upsilon_j}\right)},$$

with scale parameter ν_j and shape parameter υ_j.

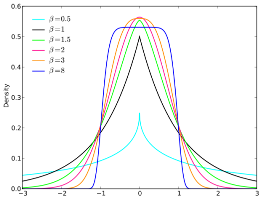

Figure: Generalised Gaussian distribution (GGD).

Learning the statistics of the CMB and string signals in wavelet space

- Require two simulated string maps: one for training; one for testing.

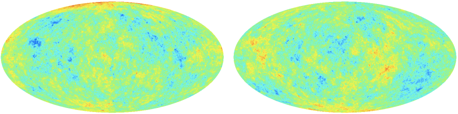

(a) String1 (b) String2

Figure: Cosmic string simulations.

- Compare distribution learnt from the training simulation (string2) with the distribution of the testing simulation (string1).
- Distributions in close agreement.

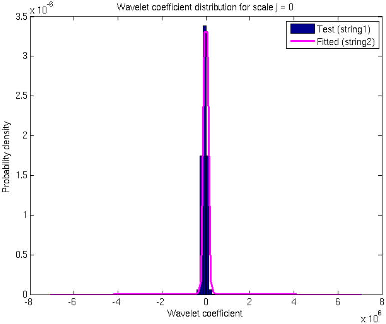

Figure: Distributions for wavelet scale $j = 0$.

Learning the statistics of the CMB and string signals in wavelet space

- Require two simulated string maps: one for training; one for testing.

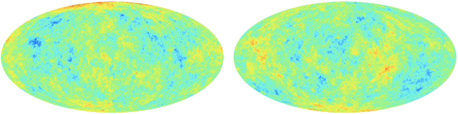

(a) String1 (b) String2

Figure: Cosmic string simulations.

- Compare distribution learnt from the training simulation (string2) with the distribution of the testing simulation (string1).
- Distributions in close agreement.

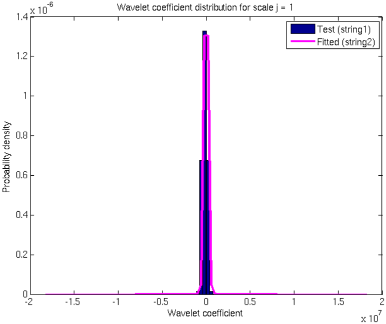

Figure: Distributions for wavelet scale $j = 1$.

Learning the statistics of the CMB and string signals in wavelet space

- Require two simulated string maps: one for training; one for testing.

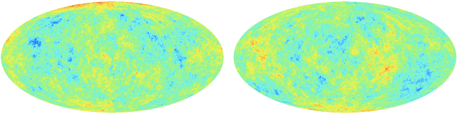

(a) String1 (b) String2

Figure: Cosmic string simulations.

- Compare distribution learnt from the training simulation (string2) with the distribution of the testing simulation (string1).
- Distributions in close agreement.

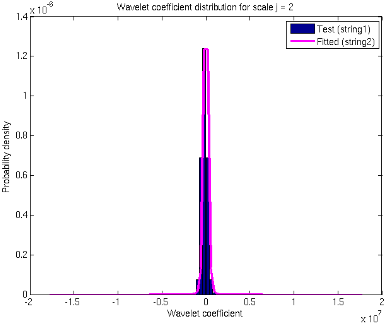

Figure: Distributions for wavelet scale $j = 2$.

Learning the statistics of the CMB and string signals in wavelet space

- Require two simulated string maps: one for training; one for testing.

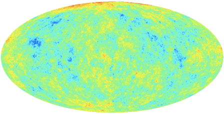

(a) String1

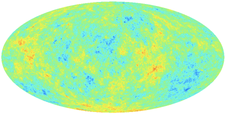

(b) String2

Figure: Cosmic string simulations.

- Compare distribution learnt from the training simulation (string2) with the distribution of the testing simulation (string1).
- Distributions in close agreement.

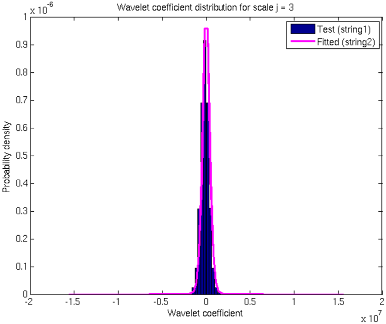

Figure: Distributions for wavelet scale $j = 3$.

Learning the statistics of the CMB and string signals in wavelet space

- Require two simulated string maps: one for training; one for testing.

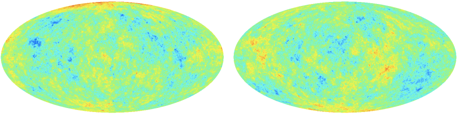

(a) String1 (b) String2

Figure: Cosmic string simulations.

- Compare distribution learnt from the training simulation (string2) with the distribution of the testing simulation (string1).
- Distributions in close agreement.

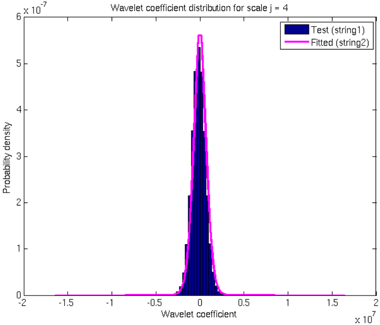

Figure: Distributions for wavelet scale $j = 4$.

Learning the statistics of the CMB and string signals in wavelet space

- Require two simulated string maps: one for training; one for testing.

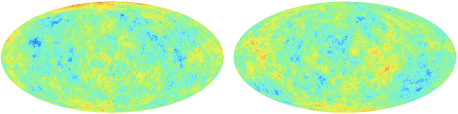

(a) String1 (b) String2

Figure: Cosmic string simulations.

- Compare distribution learnt from the training simulation (string2) with the distribution of the testing simulation (string1).
- Distributions in close agreement.
- We have accurately characterised the statistics of string signals in wavelet space.

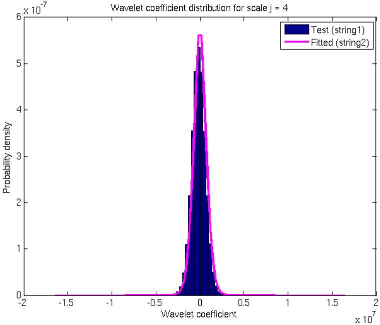

Figure: Distributions for wavelet scale $j = 4$.

Spherical wavelet-Bayesian string tension estimation

- Perform Bayesian string tension estimation in wavelet space, where the CMB and string distributions are very different.
- For each wavelet coefficient the likelihood is given by

$$\mathrm{P}(W^d_{j\rho} \mid G\mu) = \mathrm{P}(W^s_{j\rho} + W^c_{j\rho} \mid G\mu) = \int_{\mathbb{R}} \mathrm{d}W^s_{j\rho} \, \mathrm{P}^c_j(W^d_{j\rho} - W^s_{j\rho}) \, \mathrm{P}^s_j(W^s_{j\rho} \mid G\mu) \, .$$

- The overall likelihood of the data is given by

$$\mathrm{P}(W^d \mid G\mu) = \prod_{j,\rho} \mathrm{P}(W^d_{j\rho} \mid G\mu) \, ,$$

where we have assumed independence.

Spherical wavelet-Bayesian string tension estimation

- Perform Bayesian string tension estimation in wavelet space, where the CMB and string distributions are very different.
- For each wavelet coefficient the likelihood is given by

$$\mathrm{P}(W^d_{j\rho} \,|\, G\mu) = \mathrm{P}(W^s_{j\rho} + W^c_{j\rho} \,|\, G\mu) = \int_{\mathbb{R}} \mathrm{d}W^s_{j\rho} \; \mathrm{P}^c_j(W^d_{j\rho} - W^s_{j\rho}) \; \mathrm{P}^s_j(W^s_{j\rho} \,|\, G\mu) \; .$$

- The overall likelihood of the data is given by

$$\mathrm{P}(W^d \,|\, G\mu) = \prod_{j,\rho} \mathrm{P}(W^d_{j\rho} \,|\, G\mu) \; ,$$

where we have assumed independence.

Spherical wavelet-Bayesian string tension estimation

- Compute the string tension posterior $\mathrm{P}(G\mu \mid W^d)$ by Bayes theorem:

$$\mathrm{P}(G\mu \mid W^d) = \frac{\mathrm{P}(W^d \mid G\mu)\,\mathrm{P}(G\mu)}{\mathrm{P}(W^d)} \propto \mathrm{P}(W^d \mid G\mu)\,\mathrm{P}(G\mu)\ .$$

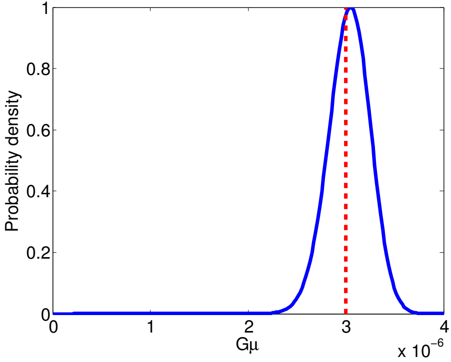

Figure: Posterior distribution of the string tension (true $G\mu = 3 \times 10^{-6}$).

Spherical wavelet-Bayesian string tension estimation

- Compute the string tension posterior $\mathrm{P}(G\mu \mid W^d)$ by Bayes theorem:

$$\mathrm{P}(G\mu \mid W^d) = \frac{\mathrm{P}(W^d \mid G\mu)\,\mathrm{P}(G\mu)}{\mathrm{P}(W^d)} \propto \mathrm{P}(W^d \mid G\mu)\,\mathrm{P}(G\mu) \, .$$

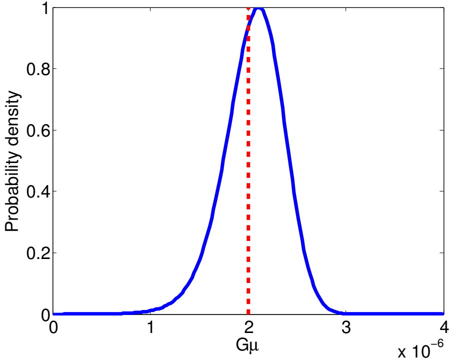

Figure: Posterior distribution of the string tension (true $G\mu = 2 \times 10^{-6}$).

Spherical wavelet-Bayesian string tension estimation

- Compute the string tension posterior $\mathrm{P}(G\mu \mid W^d)$ by Bayes theorem:

$$\mathrm{P}(G\mu \mid W^d) = \frac{\mathrm{P}(W^d \mid G\mu)\,\mathrm{P}(G\mu)}{\mathrm{P}(W^d)} \propto \mathrm{P}(W^d \mid G\mu)\,\mathrm{P}(G\mu)\;.$$

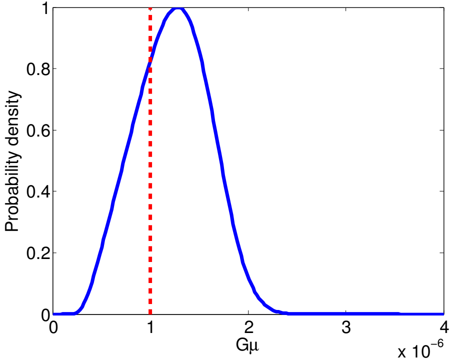

Figure: Posterior distribution of the string tension (true $G\mu = 1 \times 10^{-6}$).

Bayesian evidence for strings

- Compute Bayesian evidences to compare the string model M^s to the alternative model M^c that the observed data is comprised of just a CMB contribution.

- The Bayesian evidence of the string model is given by

$$E^s = \mathrm{P}(W^d \mid \mathrm{M}^s) = \int_{\mathbb{R}} \mathrm{d}(G\mu)\, \mathrm{P}(W^d \mid G\mu)\, \mathrm{P}(G\mu) .$$

- The Bayesian evidence of the CMB model is given by

$$E^c = \mathrm{P}(W^d \mid \mathrm{M}^c) = \prod_{j,\rho} \mathrm{P}_j^c(W_{j\rho}^d) .$$

- Compute the Bayes factor to determine the preferred model:

$$\Delta \ln E = \ln(E^s / E^c) .$$

Bayesian evidence for strings

- Compute Bayesian evidences to compare the string model M^s to the alternative model M^c that the observed data is comprised of just a CMB contribution.

- The Bayesian evidence of the string model is given by

$$E^s = \mathrm{P}(W^d \mid \mathrm{M}^s) = \int_{\mathbb{R}} \mathrm{d}(G\mu)\, \mathrm{P}(W^d \mid G\mu)\, \mathrm{P}(G\mu) \, .$$

- The Bayesian evidence of the CMB model is given by

$$E^c = \mathrm{P}(W^d \mid \mathrm{M}^c) = \prod_{j,\rho} \mathrm{P}^c_j(W^d_{j\rho}) \, .$$

- Compute the Bayes factor to determine the preferred model:

$$\Delta \ln E = \ln(E^s / E^c) \, .$$

Table: Tension estimates and log-evidence differences for simulations.

$G\mu/10^{-6}$	0.7	0.8	0.9	1.0	2.0	3.0
$\widehat{G\mu}/10^{-6}$	1.1	1.2	1.2	1.3	2.1	3.1
$\Delta \ln E$	-1.3	-1.1	-0.9	-0.7	5.5	29

Recovering string maps

- Our best inference of the wavelet coefficients of the underlying string map is encoded in the posterior probability distribution $\mathrm{P}(W^s_{j\rho} \mid W^d)$.

- Estimate the wavelet coefficients of the string map from the mean of the posterior distribution:

$$\overline{W}^s_{j\rho} = \int_{\mathbb{R}} \mathrm{d}W^s_{j\rho}\, W^s_{j\rho}\, \mathrm{P}(W^s_{j\rho} \mid W^d)$$
$$= \int_{\mathbb{R}} \mathrm{d}(G\mu)\, \mathrm{P}(G\mu \mid d)\, \overline{W}^s_{j\rho}(G\mu)\ ,$$

  where

$$\overline{W}^s_{j\rho}(G\mu) = \int_{\mathbb{R}} \mathrm{d}W^s_{j\rho}\, W^s_{j\rho}\, \mathrm{P}(W^s_{j\rho} \mid W^d_{j\rho}, G\mu)$$
$$= \frac{1}{\mathrm{P}(W^d_{j\rho} \mid G\mu)} \int_{\mathbb{R}} \mathrm{d}W^s_{j\rho}\, W^s_{j\rho}\, \mathrm{P}^c_j(W^d_{j\rho} - W^s_{j\rho})\, \mathrm{P}^s_j(W^s_{j\rho} \mid G\mu)\ .$$

- Recover the string map from its wavelets (possible since the scale-discretised wavelet transform on the sphere supports exact reconstruction).

- Work in progress. . .

Recovering string maps

- Our best inference of the wavelet coefficients of the underlying string map is encoded in the posterior probability distribution $\mathrm{P}(W^s_{j\rho} \mid W^d)$.

- Estimate the wavelet coefficients of the string map from the mean of the posterior distribution:

$$\begin{aligned}\overline{W}^s_{j\rho} &= \int_{\mathbb{R}} \mathrm{d}W^s_{j\rho}\; W^s_{j\rho}\; \mathrm{P}(W^s_{j\rho} \mid W^d) \\ &= \int_{\mathbb{R}} \mathrm{d}(G\mu)\; \mathrm{P}(G\mu \mid d)\; \overline{W}^s_{j\rho}(G\mu)\;,\end{aligned}$$

where

$$\begin{aligned}\overline{W}^s_{j\rho}(G\mu) &= \int_{\mathbb{R}} \mathrm{d}W^s_{j\rho}\; W^s_{j\rho}\; \mathrm{P}(W^s_{j\rho} \mid W^d_{j\rho}, G\mu) \\ &= \frac{1}{\mathrm{P}(W^d_{j\rho} \mid G\mu)} \int_{\mathbb{R}} \mathrm{d}W^s_{j\rho}\; W^s_{j\rho}\; \mathrm{P}^c_j(W^d_{j\rho} - W^s_{j\rho})\; \mathrm{P}^s_j(W^s_{j\rho} \mid G\mu)\;.\end{aligned}$$

- Recover the string map from its wavelets (possible since the scale-discretised wavelet transform on the sphere supports exact reconstruction).

- Work in progress...

Summary

- Observations on spherical manifolds are prevalent.
- Necessitate rigorous signal processing techniques on spherical manifolds:
  - Sampling theorems
  - Wavelets
  - Compressive sensing
- In cosmology, sensitive methods are required to extract the weak signatures of new physics from next-generation observations.